Open Access Journal

Journal of Power Technologies 97 (5) (2017) 437–445

journal homepage:papers.itc.pw.edu.pl

Operation tests of an engine supplied with alternative fuels, working as a distributed generation device

Adrian Chmielewski*, Robert Gumiński, Tomasz Mydłowski, Artur Małecki, Krzysztof Bogdziński

Warsaw University of Technology, Faculty of Automotive and Construction Machinery Engineering, Institute of Vehicles, Narbutta 84, 02–524 Warsaw, Poland

Abstract

This works discusses the test performance of a HONDA NHX 110 engine supplied with RON 95 engine fuel and alternative fuels, including: Compressed Natural Gas (CNG) and biogas. The tests were conducted for various ignition advance angle values. Tests and analyzes were performed on the basis of several hundred work cycles at maximum engine load on the authors' own low capacity, dynamometer testing unit at the Faculty of Automotive and Construction Machinery Engineering. To analyze the test results in their statistical rendering, use was made of measures such as kurtosis, coefficient of variation, asymmetric coefficient, probability density function among others. The research determined the repeatability of a performed experiment and how selected operation parameters (ignition advance angle, fuel type) influence the repeatability of measurements. The use of alternative fuels to power a low-power spark-ignition combustion engine was also analyzed in this work in the context of its use as a distributed generation device, particularly in a polygeneration system. The paper also presents and analyzes toxic compound emissions accompanying the work of the engine.

Keywords: Operation tests; alternative fuels; open indicator diagram; probability density function; distributed generation; statistical analysis

1. Introduction

The prospect of fossil fuels running out short throws a new light on how we view the functioning of the Polish and pan-European energy market. The European Union climate and energy package mandates new and old members of the Union to increase the share of renewable energy sources on the energy market (27% by 2030) and limit CO_2 emissions (by 40% by 2030, compared to 1990 levels) [1]. The climate package for 2020 [2] targets 20% share of renewable energy on the market (15% for Poland), 20% increase in energy efficiency, 20% decrease in CO_2 emissions (compared to 1990) and a mandatory minimum target of 10% of biofuels in total consumption of petrol/gasoline and diesel in transport [2]. The 20-20-20 target provides an impetus for the development of new distributed energy generation technologies [3, 4, 5, 6, 7, 8, 9, 10, 11, 12, 13, 14, 15, 16] such as devices that produce energy from renewable energy sources (RES) and devices that utilize waste heat emitted to produce electricity in one technological process (Combined Heat and Power plants—CHP [17]). In the context of energy efficiency, one area of research has concentrated on small scale cogeneration devices: microgeneration devices (producing up to 50 kW) [5, 6].

The Honda NXH 110 engine examined in this work falls in that category [3], since it can be fueled by alternative fuels [18, 19, 20, 21]. From the perspective of the end user of the Honda NXH 110, it is essential to have accurate information about long-term operation. For the purpose of determining the correct operational parameters (e.g. ignition advance angles, fuel type) this requires the acquisition of operational conditions data and the acquisition and analysis of data regarding toxic compounds generated during operation. Analysis conducted from this angle examines the effects of selected operational parameters on the amount of electricity generated by the device as well as its operational reliability [12, 16, 22, 23, 24, 25, 26] using the given fuel [27, 28, 29, 30, 31, 32, 33]. Long-term operating research can determine the expected life time of the device, which is a key concern when considering the commercial profitability of an investment in a distributed energy generation device.

The following work presents a research study of a Honda NHX low power internal combustion engine, fueled by

*Corresponding author

Email address: a.chmielewski@mechatronika.net.pl (Adrian Chmielewski)

RON 95, CNG and biogas. The structure of the work is as follows: section 2 presents and describes the engine test stand and its components, the measurement track and control system. Section 3 presents the statistical measures used for the analysis of results and sets out the range of experiments conducted. Section 4 contains the main conclusions based on the analysis of results.

2. Description of the testbed-bench

The engine test stand is presented in Fig. 1 and 2. It consists of a 4 stroke Honda NHX internal combustion engine (ICE Honda NHX), an electric machine, a programmable Engine Control Unit known as ECU Master EMU [24] (EMU—Engine Management Unit), a measurement chain and a control unit. The ICE engine was equipped with a trifunctional catalytic converter. The torque generated was received by the brushless electric motor with permanent magnets working as an electric generator. The electrical power receiving circuit consisted of a 3 phase bridge rectifier (parameters: maximum voltage: 400 V, maximum current: 300 A), a transistor module, a resistor module of 0.05 Ω resistance, brushless electric motor with permanent magnets (parameters: resistance 0.0004 Ω, voltage range: 30 to 70 V, rotational speed: 150 rpm/1 V of input voltage, maximum rotational speed (at maximum voltage value): 10500 rpm, current draw of motor with no load: 13 A at 20 V input voltage). The transistor module was controlled by a custom microprocessor controller, described in detail in [25]. To transfer the torque from the combustion engine's crankshaft to the electric generator, a toothed belt transmission was used (ratio: $i = 1.42$). The torque was measured with a Zemic L6N load cell sensor (class C3 accuracy). The crankshaft angle was measured with a digital 14 bit absolute encoder with SSI standard communication between the encoder and the measurement chain, at a rate of 44.9 kHz, which provided measurement accuracy of 0.5° of the crankshaft angle (CA) at 3800 rpm (respectively 1° CA at 7600 rpm). A detailed description of the test stand was given in [19, 20, 25, 26].

Analytical dependencies used in the analysis of results from the test stand are presented in subsection 3.1 .

3. Testbed research

3.1. Theoretical background for analysis of experimental data

The analysis regard the time of standard operation of the Honda NXH 110 engine. During analysis of selected data sets, several characteristic features of experimental data were taken into consideration, such as raw moments and central moments [34]. k-th central moments M_K will be analyzed, known as the mean deviation of the value x_i from the arithmetic mean μ:

$$M_k = \frac{1}{n}\sum_{i=1}^{n}(x_i-\mu)^k \tag{1}$$

where:
μ- arithmetic mean described by:

$$\mu = \frac{1}{n}\sum_{i=1}^{n}x_i \tag{2}$$

Another important feature of the given sample is the asymmetry coefficient S which is the 3rd central moment (w=3 in dependancy 1) divided by standard deviation cubed. It describes the asymmetry of results and can be written as:

$$S = \frac{M_3}{\sigma^3} \tag{3}$$

$S = 0$—symmetrical distribution,
$S > 0$—right-side distribution,
$S < 0$—left-side distribution.
Another measure describing the given sample is Kurtosis (Kurt). It describes the flatness of the distribution around the mean value. Kurtosis is the result of division of 4th central moment by standard deviation to the power 4. It can be written as:

$$Kurt = \frac{M_4}{\sigma^4} \tag{4}$$

If:
$K = 3$—flatness similar to normal distribution (Gaussian distribution),
$K > 3$—distribution more concentrated than normal,
$K < 3$—distribution less concentrated than normal.
Standard deviation can be expressed as follows:

$$\sigma = \sqrt{\frac{\sum_{i=1}^{n}(x_i-\mu)^2}{n}} \tag{5}$$

Coefficient of variation (CoV) between standard deviation (σ) and arithmetic mean value (μ) can be described as:

$$CoV = \frac{\sigma}{\mu} \tag{6}$$

For comparisons between research results and statistical measures, probability density function, describing the probability of a random variable appearing, is most commonly used [34].

The results of research and analysis using dependencies 1–6 for the Honda NXH 110 engine are presented in subsection 3.1.

3.2. Testbed research results

The following subsection presents the results of testbed research on the Honda NXH 110 engine. Subsection 3.2.1 contains open indicated pressure graphs for several hundred consecutive work cycles for RON 95, CNG and biogas. Presented as well are averaged pressure values for the entire work cycle, taken from several hundred work cycles. In subsection 3.2.2 probability density function graphs for ignition advance angle IAA=40° are presented. Subsection3.2.3 presents graphs of standard deviation values for IAA=10° to IAA=40° for consecutive pressure cycles, for RON 95,

Figure 1: Photo of the test stand in a climatic chamber [19, 20]

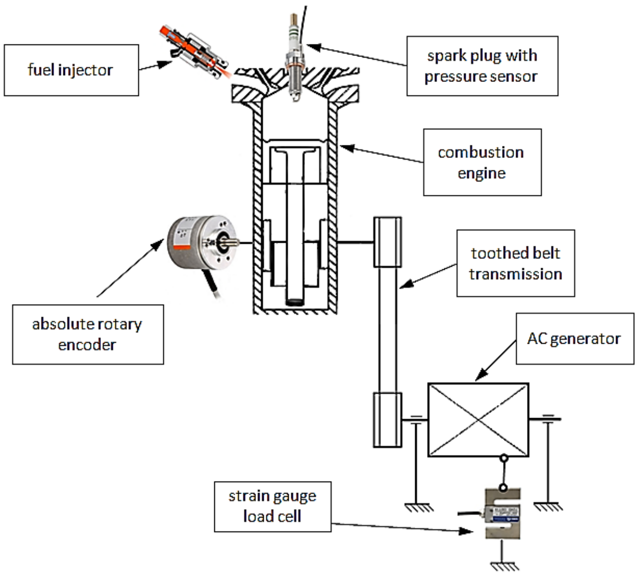

Figure 2: Schematic diagram of the test stand [19, 20]

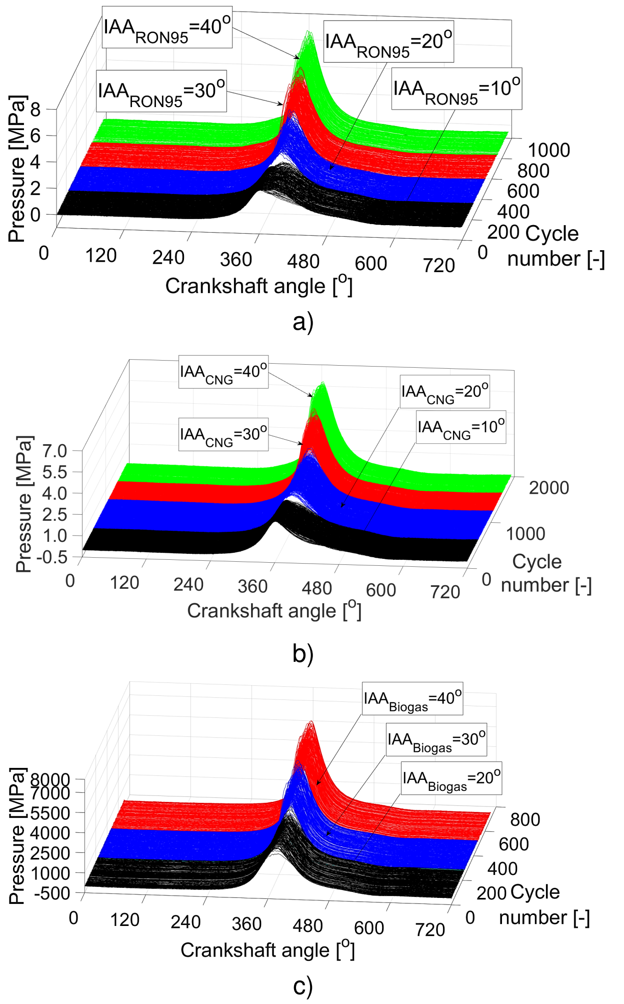

Figure 3: Open indicated pressure graphs, consecutive pressure cycles for: a) RON 95, b) CNG, c) biogas [18, 19]

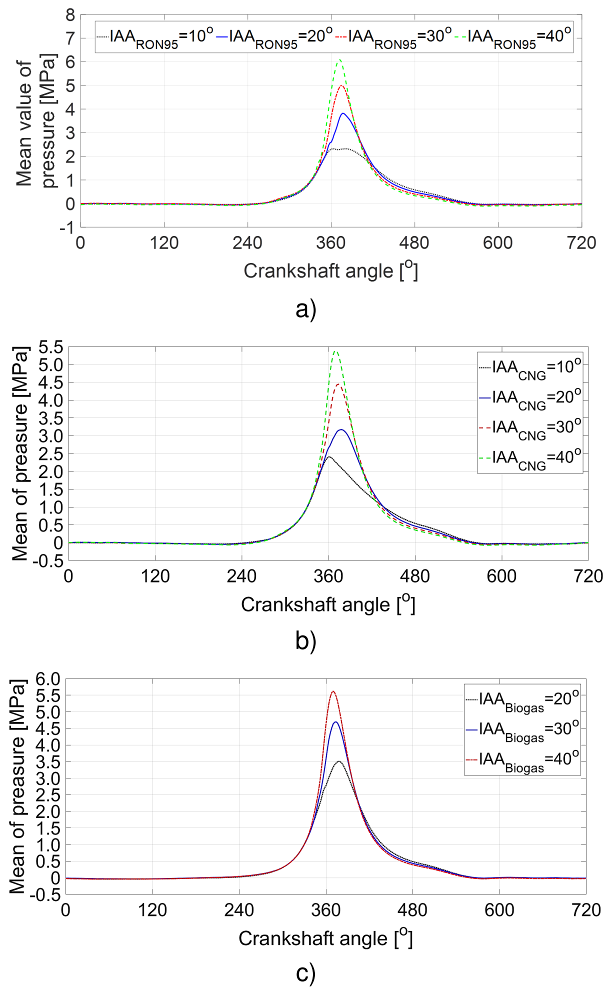

Figure 4: Open indicated pressure graphs, averaged, range from 0°CA to 720°CA for: a) RON 95, b) CNG, c) biogas [18, 19]

CNG and biogas (with IAA=20° for biogas). Subsection 3.2.4 presents graphs of Kurtosis and Skewness for consecutive cycles of indicated pressures. Subsection 3.2.5 presents graphs of electrical power and graphs of toxic compound emissions, including hydrocarbons (HC) and nitric oxides (NOx) for selected values of ignition advance angle.

3.2.1. Open indicated pressure graphs

The following section presents the effects of change of ignition advance angle (IAA) over pressure values for consecutive work cycles of the Honda NHX 110 engine, fueled by RON 95 unleaded gasoline / petrol (Fig. 3a), compressed natural gas (CNG, Fig. 3b) and biogas (Fig. 3c). For RON and CNG tests with IAA ranging from 10° to 40°, with 10° increments were conducted. For biogas, for IAA=10° operation of the engine was not possible (during tests with IAA=10° before piston Top Dead Center (TDC) operation of the engine was not stable. Engine shutdowns and misfiring events were noted). For IAA=20° to IAA=40° the engine fueled by biogas was operating correctly (Fig. 3c). It is worth noting that for all the fuels tested (Fig. 3), increase of the ignition advance angle resulted in higher pressure values inside the combustion chamber. In the works [18, 19] open pressure charts for the E85 Honda NHX 110 engine are also presented.

Figure 4 presents the effects of ignition advance angle change on a averaged open indicated pressure graph for entire cycle (average taken from several hundred cycles, including consecutive cycles as presented in Fig. 3), range from 0°CA to 720°CA for Honda NHX 110, fueled by RON 95 (Fig. 4a), CNG (Fig. 4b) and biogas (Fig. 4c). Highest averaged pressure values for range from 0°CA to 720°CA were noted at IAA=40°, as follows, for RON 95 maximum pressure was 6.09 MPa, for CNG—5.39 MPa, for biogas—5.62 MPa. Highest ignition delays were noted for IAA=40°, for RON 95 the delay was 14.3°, for CNG—23.2°, for biogas—25.1°.

3.2.2. Probability density function graphs (PDF)

In the following subsection the probability density function graphs for ignition advance angle IAA=40° were presented (Fig. 5), as follows, for RON 95 (Fig. 5a), CNG (Fig. 5b) and biogas (Fig. 5c). For all tested fuels, two areas can be highlighted: in the first one the PDF has a value above 0.01

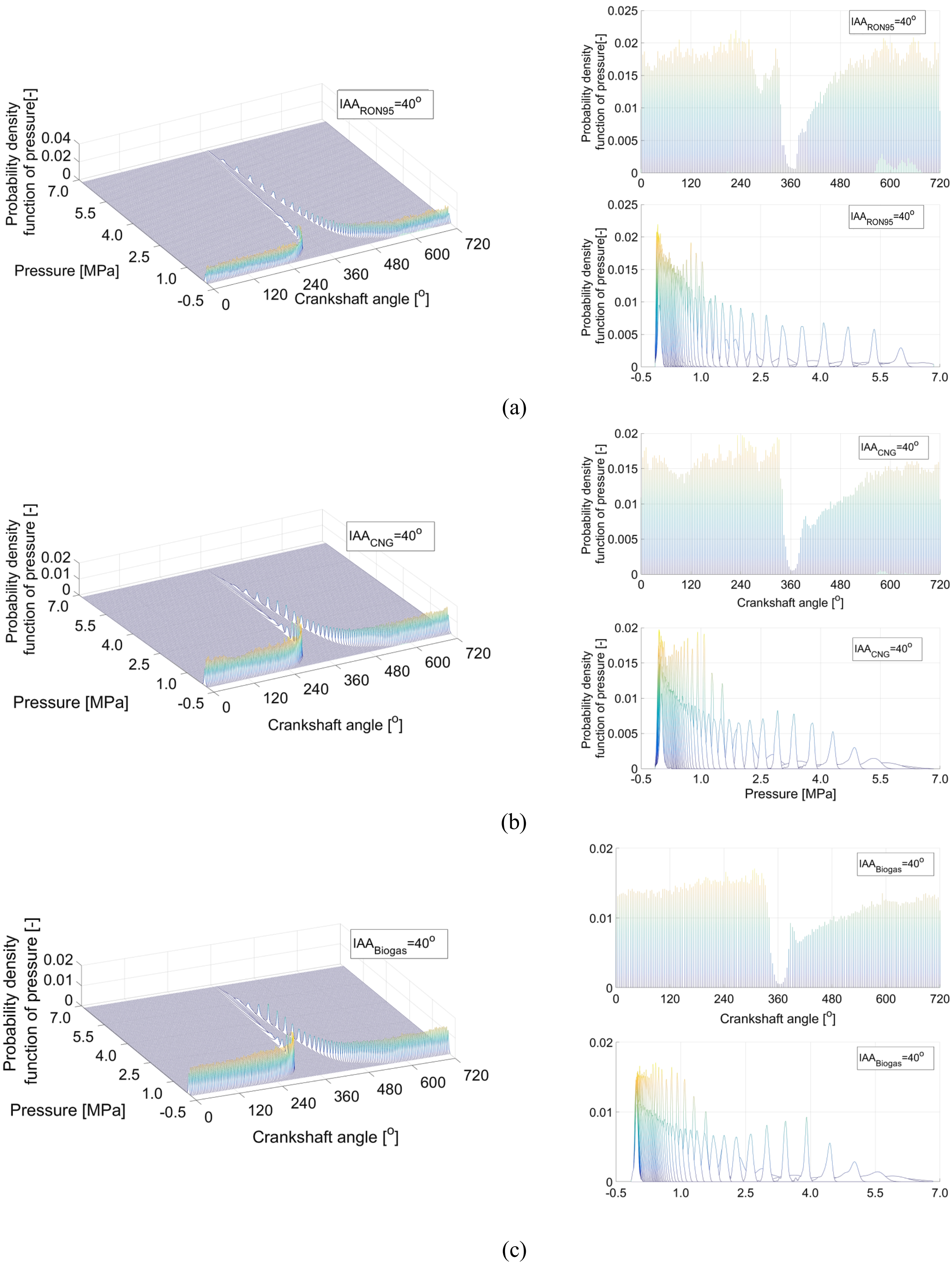

Figure 5: Probability density function graphs for: a) RON 95, b) CNG, c) biogas

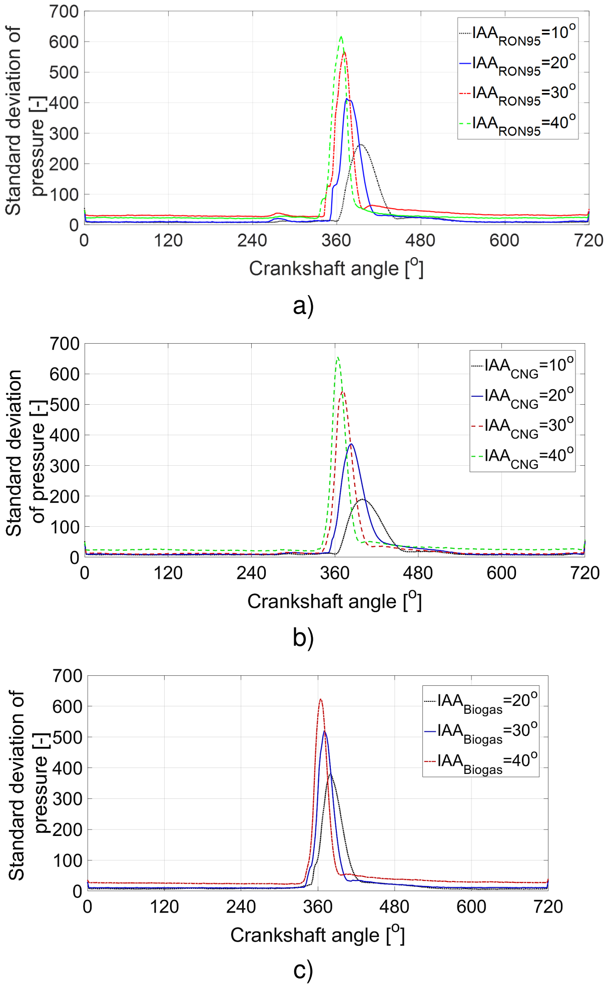

Figure 6: Standard deviation graphs for: a) RON 95, b) CNG, c) biogas

(in this area no combustion process occurs), and an area with PDF value below 0.01 (combustion processes occur, accompanied by higher dispersion of values from mean value and higher values of standard deviation—Fig. 6, greatly increased skewness values—Figures 7–9, and higher values of kurtosis—Fig.10). Higher value of probability density indicates [22, 23] greater regularity of results in area 1. Area 2 indicates that combustion processes are less regular over several hundred work cycles for all tested fuels (PDF_{min}<0.0012). Highest value PDF=0.022 was noted for RON 95 (Fig. 5a) in area 1. Lowest value PDF=0.017 was noted for biogas (Fig. 5c). Lowest value of PDF for biogas is a result of fuel contamination with carbon dioxide.

3.2.3. Standard deviation graphs

In the following subsection the effect of ignition advance angle change on standard deviation values for RON 95 (Fig. 6a), CNG (Fig. 6b) and biogas (Fig. 6c) were presented. Based on analysis of Fig. 6 it can be concluded that with increase of ignition advance angle in area where combustion processes occur (for IAA=40° respectively, for RON 95 range from 334°CA to 390°CA, for CNG range from 338°CA to 398°CA and for biogas range from 340°CA to 396°CA) increased values of standard deviation can be observed. Highest value of standard deviation occurs for CNG (655.4 at 364°CA—Fig. 6b) and biogas (623.6 at 364°CA—Fig. 6c), for RON 95 (618 at 366°CA—Fig. 6a). In other areas values of standard deviation did not exceed 65.

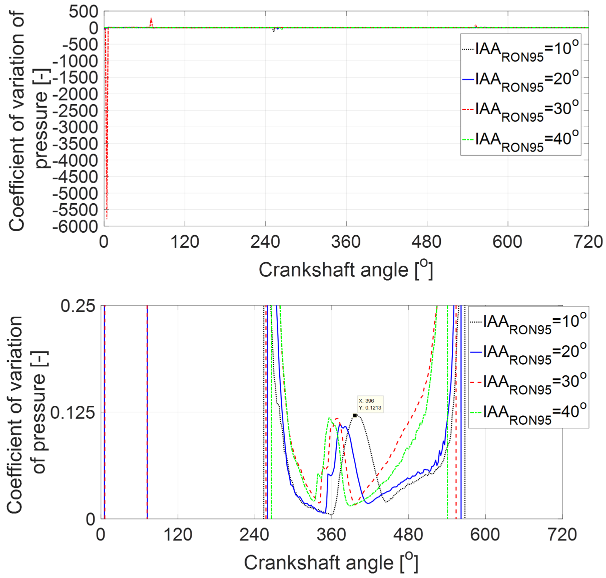

Figure 7: Coefficient of variation graph for RON 95

In Figures 7, 8, 9 effects of ignition advance angle change on coefficient of variation (CoV) were presented. Since pressure values are less than 0 beyond range 540°CA<x<240°CA high impulses occur. The range carrying information 240°CA<x<540°CA is the range in which combustion processes occur. Based on analysis of range in which combustion processes occur, an increase in CoV value can be observed, which can be used to determine precisely the ignition delay. CoV for all tested fuels in range 240°CA<x<540°CA does not exceed 0.125.

3.2.4. Skewness and kurtosis graphs

The following subsection presents the effects of ignition advance angle change on values of skewness (Fig. 10) and kurtosis (Fig. 11) for tested fuels, respectively: RON 95—skewness—Fig. 10a, kurtosis—Fig. 11a, CNG—skewness—Fig. 10b, kurtosis—Fig. 11b, biogas—skewness—Fig. 10c, kurtosis—Fig. 11c.

From analysis of Fig. 10 it can be concluded that highest values of skewness for all fuels occur in are of fuel combustion, in range 240°CA<x<540°CA [33]. Highest value of skewness can be noted for CNG for IAA=20 at -11.79 (430°CA, left-sided asymmetry). In case of RON 95 highest value of skewness appears for IAA=40°, at -3.69 (382°CA, left-sided asymmetry). In case of biogas, highest value of skewness was noted for IAA=30° at -2.54 (400°CA, left-sided asymmetry). It's worth highlighting, that for 240°CA>x>540°CA value of skewness for all tested fuels does not exceed ±0.6.

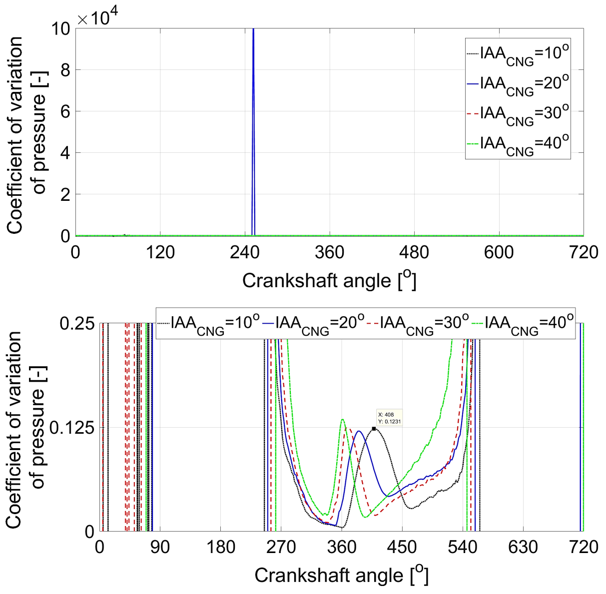

Figure 8: Coefficient of variation graph for CNG

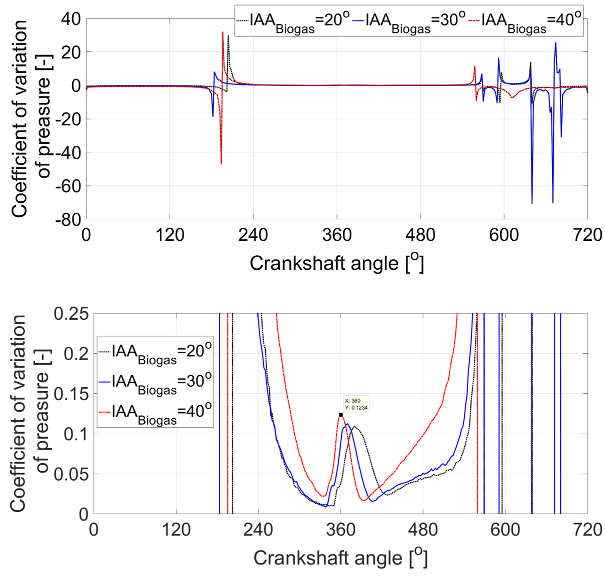

Figure 9: Coefficient of variation graph for biogas

For kurtosis, highest value was observed for CNG for IAA=20°, at 213.1 (430°CA). For RON 95 kurtosis value was 30.47 at IAA=40° and 384°CA. Highest kurtosis value for biogas was observed for IAA=30° at 13.09 (400°CA).

3.2.5. Graphs of electric power and toxic compounds emissions for alternative fuels and RON 95

In the following subsection presented are: the effects of ignition advance angle change on electrical power output, for RON 95, CNG and biogas (Fig. 12) and effects on toxic compounds (Fig. 13), such as hydrocarbons (HC) and nitric oxides (NOx) emissions of a Honda NHX 110 internal combustion engine. In the works [18, 19] the content of the CO and CO_2 of the considered fuels for the Honda NHX 110 internal combustion engine have been presented. Based on analysis of Fig. 12, it can be concluded that with increase of ignition advance angle the electrical power value increases. Respectively, the highest power output is achieved on RON 95 for IAA=30° at 4.157 kW (for IAA=40° the power value is similar, at 4.155 kW). In case of biogas and CNG, the highest power was noted for IAA=40°, respectively: 3.028 kW for biogas and 2.987 kW for CNG.

4. Summary and conclusions

In the work a research study of Honda NHX low power internal combustion engine fueled by RON 95, CNG and biogas. For data analysis typical statistical measures were used, including kurtosis, coefficient of variability, skewness, probability density function and standard deviation.

Based on conducted analysis of pressures it was concluded, that in angle range 240°CA<x<540°CA, where combustion processes occur, repetitiveness of results was not achieved. This indicates that combustion processes are accompanied by random processes, dependent on several factors, among others, heat exchange inside the combustion chamber and type of fuel.

Analysis of changes in probability density function can be used to precisely determine the combustion delay and beginning and end points of combustion. In areas where combustion processes occur, the probability density function for Honda NHX 110 engine does not exceed 0.0012.

Based on conducted research it was concluded that with increase of ignition advance angle the indicated pressure increases (for both, averaged cycle from a representative selection of several hundred cycles as well as for each measured cycle, highest values were observed at IAA=40° for all tested fuels—RON 95, CNG and biogas), this causes increase in indicated work and indicated power, net power and electrical power values. Highest value of electrical power was achieved on RON 95 for IAA=30°, at 4.157 kW (for IAA=40° value of power was similar: 4.155 kW). In case of biogas and CNG, highest electrical power was achieved for IAA=40°, respectively 3.028 kW for biogas and 2.987 kW for CNG.

Based on conducted research it was concluded that with increase of ignition advance angle, hydrocarbon emissions increase for all tested fuels. Highest values were present for IAA=40°, for RON 95 fuel the HC emission was 158 ppm, for CNG—144 ppm and for biogas it was the lowest—115 ppm. However NOx emission was highest for biogas—638 ppm, which is a direct result of higher CO_2 content. Furthermore, it was concluded that with increase of ignition advance angle NOx emission for all tested fuels increased as well. This is a result of higher pressures in the combustion chamber, and therefore, higher temperatures of combustion, which favor forming nitric oxides. Moreover, with increase of ignition advance angle the exhaust gas temperature decreased,

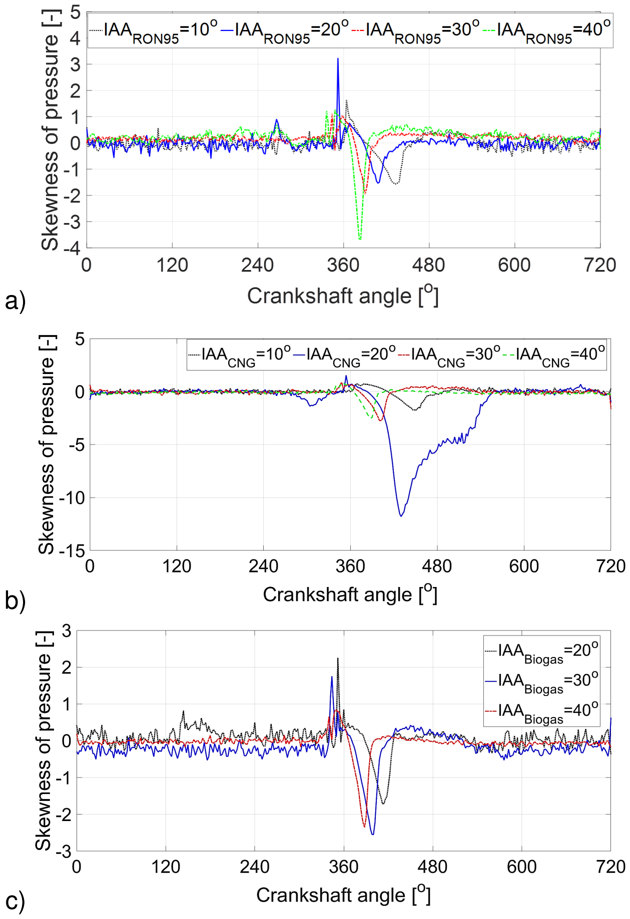

Figure 10: Graphs of skewness for: a) RON 95, b) CNG, c) biogas

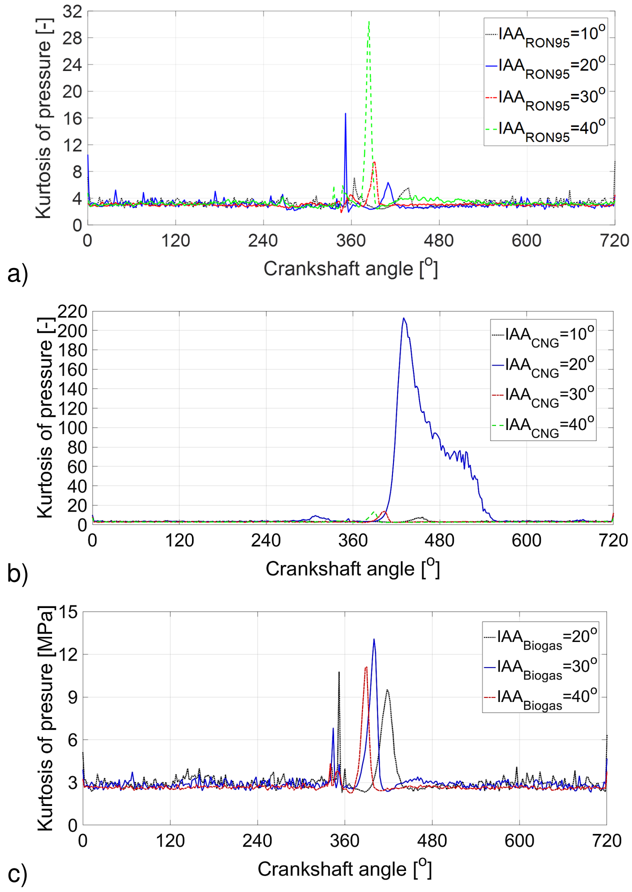

Figure 11: Graphs of kurtosis for: a) RON 95, b) CNG, c) biogas

which has a direct effect on the temperature of the catalytic converter and higher emissions of HC and other toxic substances.

References

[1] CO EUR 13 CONCL 5 (2030 CLIMATE AD EERGY POLICY FRAMEWORK), Brussels, 24 October 2014.

[2] E. Union, Directive 2009/28/ec of the european parliament and of the council of 23 april 2009 on the promotion of the use of energy from renewable sources and amending and subsequently repealing directives 2001/77/ec and 2003/30/ec, Official Journal of the European Union 5 (2009) 2009.

[3] E. E. Directive, Directive 2012/27/eu of the european parliament and of the council of 25 october 2012 on energy efficiency, amending directives 2009/125/ec and 2010/30/eu and repealing directives 2004/8/ec and 2006/32, Official Journal, L 315 (2012) 1–56.

[4] F. Martín-Martínez, A. Sánchez-Miralles, M. Rivier, C. Calvillo, Centralized vs distributed generation. a model to assess the relevance of some thermal and electric factors. application to the spanish case study., Energy.

[5] A. Chmielewski, R. Gumiński, J. Mączak, S. Radkowski, P. Szulim, Aspects of balanced development of res and distributed microcogeneration use in poland: Case study of a μchp with stirling engine, Renewable and Sustainable Energy Reviews 60 (2016) 930–952.

[6] J. Milewski, Ł. Szabłowski, J. Kuta, Control strategy for an internal combustion engine fuelled by natural gas operating in distributed generation, Energy Procedia 14 (2012) 1478–1483.

[7] J. Milewski, M. Wołowicz, Ł. Szabłowski, J. Kuta, Control strategy for a solid oxide fuel cell fueled by natural gas operating in distributed generation, Energy Procedia 29 (2012) 676–682.

[8] A. Chmielewski, R. Gumiński, J. Mączak, Selected properties of the adiabatic model of the stirling engine combined with the model of the piston-crankshaft system, in: Methods and Models in Automation and Robotics (MMAR), 2016 21st International Conference on, IEEE, 2016, pp. 543–548.

[9] J. R. Horne, M. Carreras-Sospedra, D. Dabdub, P. Lemar, U. Nopmongcol, T. Shah, G. Yarwood, D. Young, S. L. Shaw, E. M. Knipping, Air quality impacts of projections of natural gas-fired distributed generation, Atmospheric Environment 168 (2017) 8–22.

[10] A. A. Chmielewski, R. Guminski, J. Maczak, P. Szulim, Model-based research on a micro cogeneration system with stirling engine, Journal of Power Technologies 96 (4) (2016) 295.

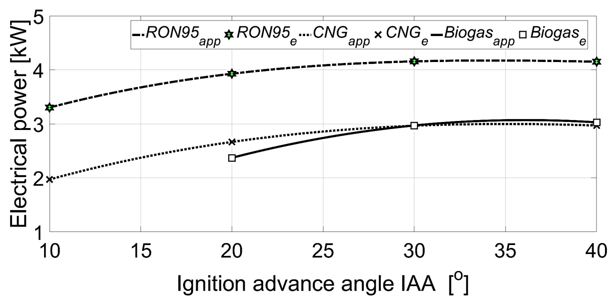

Figure 12: Graphs of electrical power for: RON 95, CNG and biogas

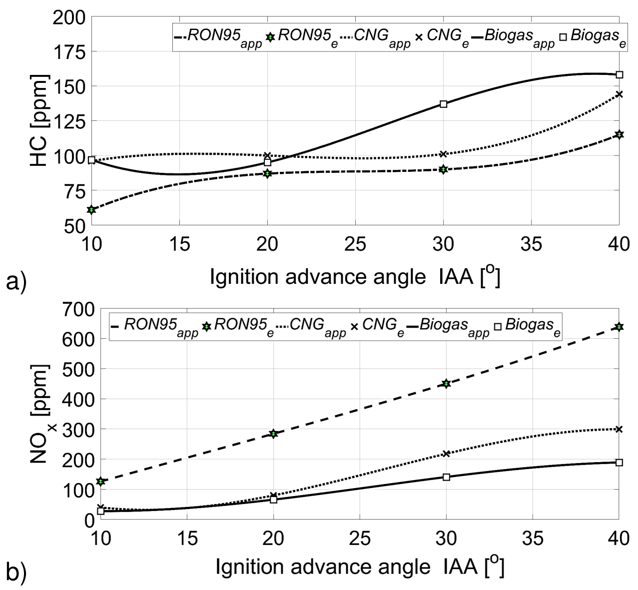

Figure 13: Graphs of emissions: a) HC, b) NOx, for RON 95, CNG and biogas

[11] J. Milewski, G. Discepoli, U. Desideri, Modeling the performance of mcfc for various fuel and oxidant compositions, International Journal of Hydrogen Energy 39 (22) (2014) 11713–11721.

[12] A. Chmielewski, S. Gontarz, R. Gumiński, J. Mączak, P. Szulim, Research study of the micro cogeneration system with automatic loading unit, in: Challenges in Automation, Robotics and Measurement Techniques, Springer, 2016, pp. 375–386.

[13] L. Szablowski, J. Milewski, J. Kuta, K. Badyda, Control strategy of a natural gas fuelled piston engine working in distributed generation system, Rynek Energii (3) (2011) 33–40.

[14] A. Chmielewski, R. Gumiński, J. Mączak, Selected properties of the dynamic model of the piston-crankshaft assembly in stirling engine combined with the thermodynamic submodel, International Journal of Structural Stability and Dynamics (2017) 1740009.

[15] J. Dong, T.-t. Feng, H.-x. Sun, H.-x. Cai, R. Li, Y. Yang, Clean distributed generation in china: Policy options and international experience, Renewable and Sustainable Energy Reviews 57 (2016) 753–764.

[16] A. Chmielewski, S. Gontarz, R. Gumiński, J. Mączak, P. Szulim, Research on a micro cogeneration system with an automatic load-applying entity, in: Challenges in Automation, Robotics and Measurement Techniques, Springer, 2016, pp. 387–395.

[17] E. Directive, Directive 2004/8/ec of the european parliament and of the council of 11 february 2004 on the promotion of cogeneration based on a useful heat demand in the internal energy market and amending directive 92/42/eec, Official Journal of the European Union (2004) 50–60.

[18] C. Bae, J. Kim, Alternative fuels for internal combustion engines, Proceedings of the Combustion Institute 36 (3) (2017) 3389–3413.

[19] A. Chmielewski, R. Gumiński, T. Mydłowski, A. Małecki, K. Bogdziński, Research study of honda nhx 110 powered by an alternative fuel, in: 2nd International Conference on the Sustainable Energy and Environment Development – SEED'17 IOP Conference Series: Energy and Enviromental Studies [In print], 2017.

[20] A. Chmielewski, R. Gumiński, T. Mydłowski, A. Małecki, K. Bogdziński, Research on honda nhx 110 fueled with biogas, cng and e85, in: 2nd International Conference on the Sustainable Energy and Environment Development – SEED'17 IOP Conference Series: Energy and Enviromental Studies [In print], 2017.

[21] F. Yan, L. Xu, Y. Wang, Application of hydrogen enriched natural gas in spark ignition ic engines: from fundamental fuel properties to engine performances and emissions, Renewable and Sustainable Energy Reviews.

[22] A. Chmielewski, S. Gontarz, R. Gumiński, J. Mączak, P. Szulim, Analiza wpływu parametrów eksploatacyjnych na drgania układu mikrokogeneracyjnego, Przegląd Elektrotechniczny 92 (1) (2016) 45–53.

[23] A. Chmielewski, R. Gumiński, J. Mączak, P. Szulim, Badania układu mikrokogeneracyjnego z silnikiem stirlinga. część ii, Rynek Energii (5) (2015) 120.

[24] A. Małecki, T. Mydłowski, S. Radkowski, Przegląd uniwersalnych sterowników do silników zi, ZESZYTY NAUKOWE INSTYTUTU POJAZDÓW 2 (2013) 93.

[25] J. Dybała, T. Mydłowski, A. Małecki, K. Bogdziński, Stanowisko hamowniane do badań silników spalinowych o małych mocach, Combustion Engines 54 (3) (2015) 996–1000.

[26] A. Małecki, T. Mydłowski, J. Dybała, Badania wpływu zanieczyszczeń biopaliw na sprawność silnika zi, ZESZYTY NAUKOWE INSTYTUTU POJAZDÓW 3 (2014) 99.

[27] M. M. N. de Faria, J. P. V. M. Bueno, S. M. E. Ayad, C. R. P. Belchior, Thermodynamic simulation model for predicting the performance of spark ignition engines using biogas as fuel, Energy Conversion and Management 149 (2017) 1096–1108.

[28] Y.-Y. Wu, B.-C. Chen, F.-C. Hsieh, C.-T. Ke, Heat transfer model for small-scale spark-ignition engines, International Journal of Heat and Mass Transfer 52 (7) (2009) 1875–1886.

[29] M. M. Nunes, J. P. V. M. Bueno, S. M. E. Ayad, C. R. P. Belchior, Thermodynamic simulation model for predicting the performance of spark ignition engines using biogas as fuel, Energy Conversion and Management.

[30] Z. Chłopek, J. Biedrzycki, J. Lasocki, P. Wojcik, Assessment of the impact of dynamic states of an internal combustion engine on its operational properties, Eksploatacja i Niezawodność 17 (1).

[31] A. Matuszewska, M. Owczuk, A. Zamojska-Jaroszewicz, J. Jakubiak-Lasocka, J. Lasocki, P. Orliński, Evaluation of the biological methane potential of various feedstock for the production of biogas to supply agricultural tractors, Energy Conversion and Management 125 (2016) 309–319.

[32] J. Lasocki, K. Kołodziejczyk, A. Matuszewska, Laboratory-scale investigation of biogas treatment by removal of hydrogen sulfide and carbon dioxide., Polish Journal of Environmental Studies 24 (3).

[33] T. Rychter, A. Teodorczyk, Teoria silników tłokowych, Wydawnictwa Komunikacji i Łączności, 2006.

[34] W. Krysicki, J. Bartos, W. Dyczka, K. Królikowska, M. Wasilewski, Rachunek prawdopodobieństwa i statystyka matematyczna w zadaniach (2003).